Available online at www.sciencedirect.com
SCIENCE DIRECT®
Journal of Solid State Chemistry 179 (2006) 2158–2163
JOURNAL OF SOLID STATE CHEMISTRY
www.elsevier.com/locate/jssc

Thermoelectric and structural properties of a new Chevrel phase: $Ti_{0.3}Mo_5RuSe_8$

Michael A. McGuire[a], Anneliese M. Schmidt[a,1], Franck Gascoin[b,2], G. Jeffrey Snyder[b], Francis J. DiSalvo[c,*]

[a]Department of Physics, Clark Hall, Cornell University, Ithaca, NY 14853, USA
[b]California Institute of Technology – Jet Propulsion Laboratory, Pasadena, CA 91109, USA
[c]Department of Chemistry and Chemical Biology, Baker Laboratory, Cornell University, Ithaca, NY 14853, USA

Received 24 March 2006; received in revised form 12 April 2006; accepted 16 April 2006
Available online 25 April 2006

Abstract

The new Chevrel phase $Ti_{0.3}Mo_5RuSe_8$ has been synthesized and characterized by quantitative microprobe analysis, powder X-ray diffraction, and high-temperature thermoelectric properties measurements. The thermoelectric properties of this compound are compared to the previously reported data for other related Chevrel phases. We report also the results of Rietveld analysis of powder X-ray diffraction data for $Ti_{0.3}Mo_5RuSe_8$. This compound adopts the rhombohedral Chevrel phase structure (space group $R\bar{3}$, $Z = 3$) with hexagonal lattice constants $a = 9.75430(25)$ Å and $c = 10.79064(40)$ Å. The low level of incorporation and low scattering power of Ti precluded the identification of the Ti positions, and Rietveld refinement was carried out only for the Mo_5RuSe_8 framework of $Ti_{0.3}Mo_5RuSe_8$ ($R_p = 10.5\%$, $R_{wp} = 14.6\%$). Rietveld analysis was also used to refine the structure of the unfilled phase Mo_5RuSe_8 ($R\bar{3}$, $Z = 3$, $a = 9.63994(8)$ Å, $c = 10.97191(11)$ Å, $R_p = 8.0\%$, $R_{wp} = 10.5\%$). Comparisons between the two structures are made.

Keywords: Chevrel phase; Titanium molybdenum ruthenium selenide; Molybdenum ruthenium selenide; Thermoelectric; Electrical resistivity; Seebeck coefficient; Powder X-ray diffraction; Rietveld refinement

1. Introduction

Chevrel phase materials are a class of compounds whose structures are composed of a three-dimensional network of pseudo-cubic Mo_6Q_8 ($Q = S$, Se, Te) clusters, joined together through intercluster Mo–Q bonding (Fig. 1). First reported in 1971 [1], this family of materials now has many members, due to the remarkable versatility of the crystal structure [2]. The manner in which the clusters pack leaves interconnected cavities or channels throughout the structure, into which many different elements can be intercalated. In addition, other transition metals (like Ru, Rh, Re) can be substituted for Mo, and the chalcogens can be partially replaced by halogens. These fillings and substitutions can be used to tune the electronic behavior of these compounds, from the metallic parent compounds Mo_6Q_8 to the semiconducting materials $Mo_4Ru_2Se_8$ [3], $Mo_2Re_4Se_8$ [4], and $Ti_{0.9}Mo_6Se_8$ [5].

Each of the semiconducting compounds listed above has four, or nearly four, more valence electrons per cluster than Mo_6Se_8. Indeed, molecular orbital calculations on the Mo_6Q_8 cluster [6], as well as electronic band structure calculations on the extended structure [7], predict that the conduction band of Mo_6Q_8 will be filled by the addition of four electrons. The total number of valence electrons per Mo_6 cluster has been termed the cluster metal electron count (MEC) by some and the valence electron count (VEC) [8] by others. For Mo_6Se_8 VEC = 20, since the six Mo atoms have a total of 36 valence electrons, and the eight (formally 2-) Se atoms remove 16. Thus, a VEC of 24 electrons per cluster should correspond to a semiconducting compound. Interest in semiconducting Chevrel phases

*Corresponding author. Fax: +1 607 255 4137.
E-mail address: fjd3@cornell.edu (F.J. DiSalvo).
[1]Current address: Antares Group, Inc., Landover, MD, USA.
[2]Current address: Laboratoire de Physico-Chimie de la Matière Condensée, LPMC UMR-CNRS 5617, Université Montpellier 2, France.

0022-4596/$ - see front matter © 2006 Elsevier Inc. All rights reserved.
doi:10.1016/j.jssc.2006.04.022

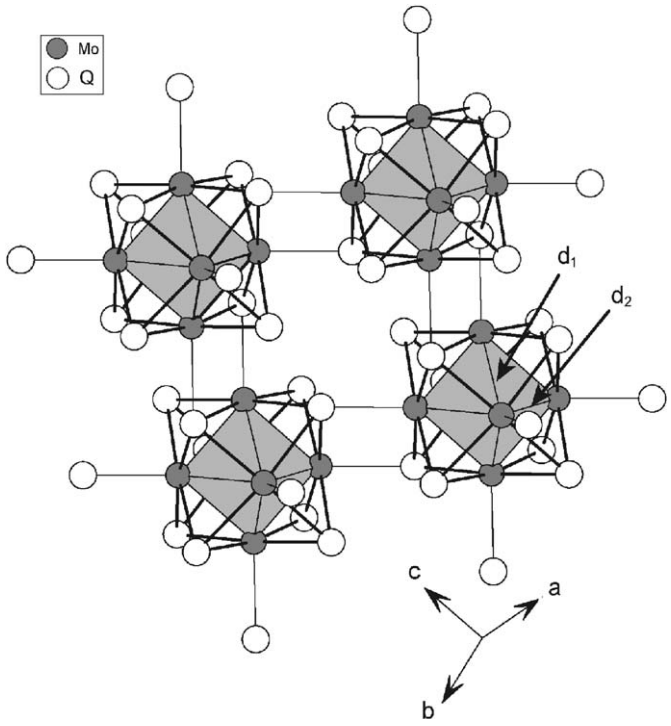

Fig. 1. A view of the Chevrel phase structure, showing how the Mo_6Q_8 units are interconnected into a three-dimensional network. The hexagonal unit cell axes and the two unique metal–metal bonds d_1 and d_2 are labeled.

recently has increased, due to the discovery of promising thermoelectric properties at high temperatures [5]. Chevrel phases are now candidate materials for use in segmented thermoelectric power generation devices.

In a thermoelectric generator, heat flow through a thermoelectric material is converted directly into electrical current [9]. The maximum conversion efficiency for a particular material is a monotonically increasing function of the dimensionless thermoelectric figure of merit $ZT = S^2T/\rho\kappa$, where T is the absolute temperature, S is the Seebeck coefficient or thermopower, ρ is the electrical resistivity, and κ is the thermal conductivity [9]. The actual efficiency is a function of the current at which the device is operated. The optimal current depends on S, ρ, and κ, and therefore varies from one material to another, and also with temperature. This must be considered when constructing a segmented thermoelectric device, where different materials are connected in series and the same current flows through each. This problem, termed thermoelectric compatibility, can have a significant impact on the overall efficiency of a power generation device operating over a large temperature range [10,11]. At absolute temperature T, the compatibility factor s (with units of V^{-1}) is defined as

$$s = \frac{\sqrt{1+ZT}-1}{ST}. \quad (1)$$

In Eq. (1), ZT is the dimensionless thermoelectric figure of merit defined above, and S is the Seebeck coefficient. It has recently been found that near 1000 °C Chevrel phases can be more compatible with the lower temperature materials than the currently used SiGe alloys, while maintaining reasonably high values of ZT [11].

The best Chevrel phase thermoelectric material discovered to date is $Cu_{3.1}Mo_6Se_8$ [5], often denoted as "$Cu_4Mo_6Se_8$". Although this compound does not show semiconducting behavior (VEC = 23.1), it has ZT near 0.6 at 1000 °C (p-type SiGe has ZT near 0.4 at this temperature [12]). However, the best thermoelectric materials are usually heavily doped semiconductors with carrier concentrations of 10^{19}–$10^{20}\,cm^{-3}$ [9]. $Cu_{3.1}Mo_6Se_8$ has a carrier concentration of $8.8\times10^{21}\,cm^{-3}$ [5]. Because of the low Seebeck coefficient at this high carrier concentration, better Chevrel phase thermoelectric materials are expected if the carrier concentration can be decreased from this value. There is also some concern that the ionic mobility of Cu^{1+} ions through the channels in the Chevrel phase structure may lead to degradation of the material under operating conditions. Thus, it is important that the thermoelectric properties of Chevrel phases with filling atoms other than Cu be investigated.

We have been using a combination of filling atoms and cluster metal substitutions to search for new Chevrel phases for thermoelectric applications. In this paper, we report results from our investigations into the Ti filling of the mixed metal cluster phase Mo_5RuSe_8. We present structural properties of Mo_5RuSe_8 and $Ti_{0.3}Mo_5RuSe_8$ based on Rietveld analysis of powder X-ray diffraction data, as well as measured high temperature thermoelectric properties of the Ti-filled phase.

2. Experimental

Mo_5RuSe_8 was obtained by deintercalation of $CuMo_5RuSe_8$, which had been made by reacting a mixture of stoichiometric amounts of the elements in sealed, evacuated, silica tubes. The mixture was first reacted at 400 °C for 1 day, mixed by shaking the unopened tube, and then heated at 1100 °C for 2 days. The product was ground, pressed into a pellet, and then annealed twice for 3 days each at 1200 °C. The sample was reground and pressed into a pellet between the two anneals. For annealing at 1200 °C, the sample was sealed in a silica tube which was then sealed in a second, larger diameter silica tube. The deintercalation was carried out by reacting $CuMo_5RuSe_8$ with iodine dissolved in acetonitrile [13]. We produce Mo_5RuSe_8 through this deintercalation method because we have found that the amount of the $MoSe_2$ impurity in the final product is lower than when Mo_5RuSe_8 is synthesized directly from the elements. This may be due to Mo self-intercalation, to which similar behavior has been attributed in $Mo_6S_{8-x}Se_x$ [14].

The deintercalation product was then used for powder X-ray diffraction studies, and as a starting material for synthesis of the Ti-filled phase. Since one-half of a Ti^{4+} ion per Mo_5RuSe_8 cluster would be needed to give a VEC of 24, the target stoichiometry of the Ti-filled phase was $Ti_{0.5}Mo_5RuSe_8$. A 1:2 molar ratio of Ti powder and

Mo_5RuSe_8 was pressed into a pellet, sealed in an evacuated silica tube, and heated at 1100 °C for 48 h. The product was ground thoroughly, pressed into a pellet, and sealed in a silica tube. This tube was then sealed under vacuum in a second silica tube, and heated at 1200 °C for 48 h. The resulting product was then used for X-ray diffraction studies, electron microprobe analysis, and high temperature thermoelectric properties measurements.

Powder X-ray diffraction patterns were recorded with a Scintag 2000 theta-theta diffractometer, using Cu$K\alpha$ radiation. Rietveld analysis was carried out using the program FULLPROF [15]. Data used for Rietveld analysis were collected in step mode, with a counting time of 6 s per 0.02° step, using an internal Si standard. In each case, three phases were refined: the Chevrel phase, the internal Si standard, and the $MoSe_2$ impurity. Refined parameters include: zero offset, asymmetry, background polynomials, scale factors, peak shapes, half-width parameters, lattice constants, displacement parameters, atomic coordinates, and preferred orientation (for $MoSe_2$ only). The Mo:Ru ratio was fixed at 5:1 in the refinements. Due to weak reflections (~1% of the height of the strongest Chevrel phase reflection) from unidentified impurities, two small regions (each about 1° wide) were excluded from the refinement for Mo_5RuSe_8.

Electron microprobe analysis of the Ti-filled phase was performed on a piece broken away from the pellet after the 1200 °C anneal. The sample was mounted in conducting epoxy, and polished using 1200 grit SiC paper followed by a 1 μm diamond suspension on a Struers Rotopol–Rotoforce polishing system. Approximately 250 Å of carbon was evaporated onto the surface after polishing. Quantitative analyses of wavelength dispersive spectra were performed using pure elemental standards prepared in a similar fashion. Measurements were carried out in a JEOL 8900 electron microprobe, operating at 15 kV and ~20 nA. Data were collected on grains which were at least 5 μm in size.

To prepare dense samples for property measurements, a finely ground polycrystalline powder of $Ti_{0.3}Mo_5RuSe_8$ was pressed at 1223 K at a pressure of about 20,000 psi for 1.5 h under an argon atmosphere in high-density graphite dies (POCO HPD-1). The measured density of the resulting pellet was about 95% of the theoretical density. Van der Pauw resistivity measurements were performed on a 1 mm thick slice of the pellet using a current of 100 mA in a special high-temperature apparatus [16]. The thermopower measurement was performed on the remaining cylinder using a high temperature light pulse technique [17]. The measurements were performed as a function of temperature from room temperature to about 1200 K.

3. Results

3.1. Microprobe analysis

Electron microprobe analysis showed that in addition to the Chevrel phase, small amounts of $MoSe_2$, $TiSe_2$, and TiO_x were also present in the sample. Based on observations made in composition mode, it is estimated that the sample was approximately 90–95% Chevrel phase. Composition data from 10 different Chevrel phase grains were normalized to give a total of six cluster metal atoms (Mo + Ru) per formula unit, and then averaged. The uncertainty on the average composition was estimated as the standard deviation of the normalized measurements. This analysis gave an average composition (with estimated uncertainties in parentheses) of $Ti_{0.28(2)}Mo_{5.08(2)}Ru_{0.92(2)}Se_{7.81(19)}$.

Clearly, not all of the Ti was incorporated into the Chevrel phase. This is consistent with the observation of Ti containing impurities ($TiSe_2$ and TiO_x) in the sample. We are unsure of the origin of the discrepancy between the measured Mo:Ru ratio and the expected ratio of 5:1. It may be a systematic error associated with the microprobe analysis, or signify the presence of an undetected Ru containing phase in the sample. We attribute the low Se content to a small amount of oxygen for selenium substitution, which has been observed in several Chevrel phases [18], and is likely to occur in silica tubes at 1200 °C since the vapor pressures of SiO and O_2 are expected to be $\sim 10^{-6}$ Torr [19]. Low Se content could also be caused by Se vacancies, which could be related to the incomplete filling observed in many Chevrel phase compounds, since fewer additional electrons would be needed to reach a semiconducting state [20].

3.2. Powder X-ray diffraction and crystal structures

The powder X-ray diffraction results for both Mo_5RuSe_8 and $Ti_{0.3}Mo_5RuSe_8$ are shown in Fig. 2. Both compounds adopt the classic Chevrel phase structure (space group $R\bar{3}$). Agreement factors and refined unit cell parameters for the Chevrel phases are shown in Table 1. The unit cell parameters for Mo_5RuSe_8 in Table 1 agree well with those reported in the literature ($a = 9.638$ Å, $c = 10.971$ Å) [21]. Atomic positions (in the hexagonal setting) are listed in Table 2. The Mo/Ru site and the site occupied by Se(1) are at Wyckoff positions 6*f* (x, y, z), while Se(2) is at Wyckoff position 2*c* (0, 0, z). The low level of incorporation of Ti, the possibility that it partially occupies several different sites, and its relatively low scattering power precluded the determination of the Ti positions using the present data. Many different locations have been observed for transition metals in the cavities of Chevrel phase structures [2,22,23]. In each case the transition metal atoms are disordered over several positions within the unit cell. Such disorder would further dilute the already small scattering power of the Ti atoms, adding to the difficulty in locating the Ti using powder X-ray diffraction methods. Only the Mo_5RuSe_8 framework has been refined for the Ti-filled phase, which may be partly responsible for the somewhat higher *R*-factors when compared to Mo_5RuSe_8.

Although the Ti atoms could not be located using the X-ray diffraction data, evidence of its incorporation is

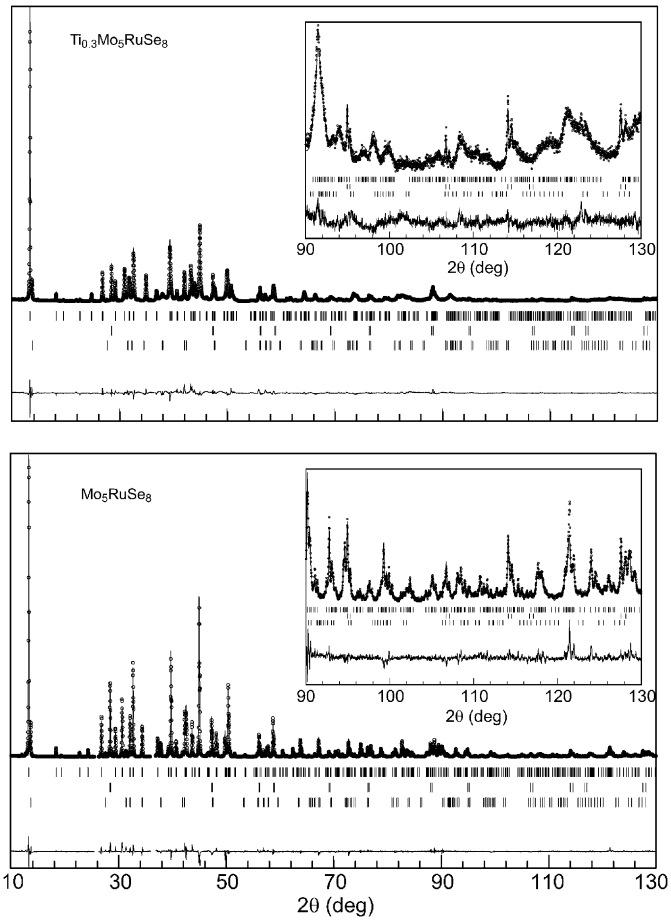

Fig. 2. Results from the Rietveld refinements for $Ti_{0.3}Mo_5RuSe_8$ and Mo_5RuSe_8, including expanded views of the high angle data, showing the measured data (circles) and calculated data (solid line). The difference curves are shown at the bottoms, and the tick marks indicate the position of the Bragg peaks for the Chevrel phases, Si, and $MoSe_2$, from top to bottom.

Table 1
Rietveld refinement results

	Mo_5RuSe_8	$Ti_{0.3}Mo_5RuSe_8$
a_H (Å)	9.63994(8)	9.75430(25)
c_H (Å)	10.97191(11)	10.79064(40)
V_H (Å^3)	883.001(13)	889.140(46)
R_p	8.04	10.4
R_{wp}	10.5	14.2
S	2.93	3.59
R_{Bragg} (Chevrel)	6.40	6.11

seen. The primitive unit cell volume of the Ti-filled phase is 2.05 Å^3 larger than that of the unfilled phase. This corresponds to an increase of 6.8 Å^3 per Ti atom. This increase is similar to the behavior seen in $Ti_{0.88}Mo_6Se_8$ (with a slightly distorted triclinic Chevrel phase structure [22]) in which the volume increases by 7.3 Å^3 per Ti atom over that of Mo_6Se_8 [24].

Table 2
Refined fractional coordinates in the hexagonal setting

	Mo_5RuSe_8	$Ti_{0.3}Mo_5RuSe_8$
Mo/Ru		
x	0.01723(16)	0.01885(25)
y	0.16789(15)	0.16703(19)
z	0.39575(13)	0.39651(20)
Se(1)		
x	0.32335(21)	0.32349(30)
y	0.28474(18)	0.28353(28)
z	0.41394(15)	0.40874(30)
Se(2)		
z	0.21499(26)	0.20900(42)

Table 3
Interatomic distances (Å), M = Mo/Ru

	Mo_5RuSe_8	$Ti_{0.3}Mo_5RuSe_8$
M–*M* (d_1)	2.671(1)	2.677(2)
M–*M* (d_2)	2.759(2)	2.716(3)
M–Se (intracluster)	2.512(3)	2.545(4)
	2.518(2)	2.546(4)
	2.537(2)	2.568(4)
	2.587(2)	2.601(4)
M–Se (intercluster)	2.621(2)	2.621(4)

The effects of the Ti on the interatomic distances in the Chevrel phase framework (Fig. 1) are also apparent. These distances are listed in Table 3. There are two metal–metal distances in the Chevrel phase cluster, d_1 (roughly parallel to the hexagonal *c*-axis) and d_2 (roughly perpendicular to the hexagonal *c*-axis). In going from Mo_5RuSe_8 to $Ti_{0.3}Mo_5RuSe_8$, d_1 increases, while d_2 decreases. It is usually the case for Chevrel phase sulfides and selenides that, as electrons are added to cluster (filling metal–metal bonding states and approaching a VEC of 24), the intracluster bonds become shorter and its shape becomes more regular [25]. The behavior observed here in $Ti_{0.3}Mo_5RuSe_8$ is consistent with these general rules. The average intracluster metal–metal distance decreases upon addition of Ti, from 2.715 to 2.697 Å. The cluster also become more regular; the difference between d_2 and d_1 decreases from 0.088 to 0.039 Å. It is also clear from Table 3 that the intercluster Mo/Ru–Se distances are increased by the addition of Ti. This is consistent with previous observation of the effect of reducing the Mo cluster core (through the introduction of filling atoms) on these distances [25].

3.3. Thermoelectric properties

Fig. 3 shows the measured electrical resistivity and thermopower of $Ti_{0.3}Mo_5RuSe_8$, and the thermoelectric power factor (PF) calculated from these measurements. The PF is defined as $PF = S^2/\rho$, and is thus closely related

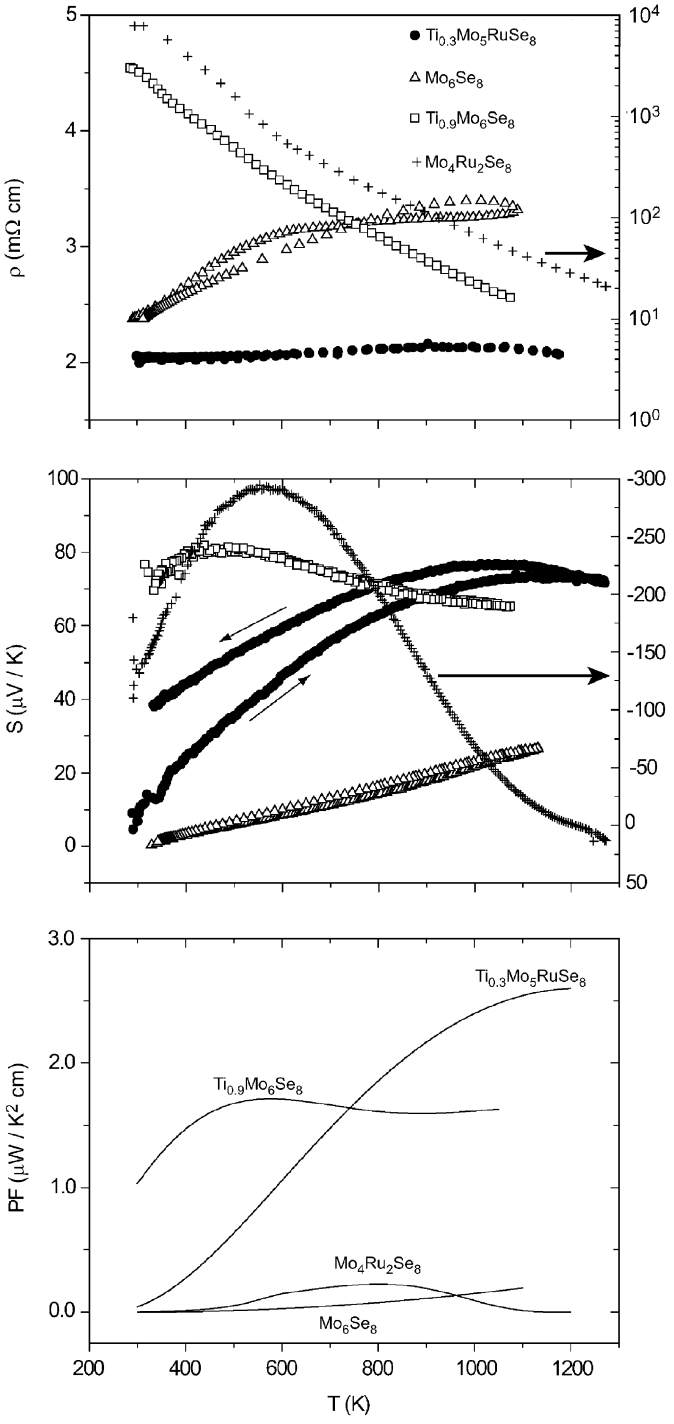

Fig. 3. The resistivity (ρ), thermopower (S) and power factor (PF) of $Ti_{0.3}Mo_5RuSe_8$, along with data from Mo_6Se_8 [5], $Ti_{0.9}Mo_6Se_8$ [5], and $Mo_4Ru_2Se_8$ [27] for comparison. Note the different scales (at right) for the resistivity and thermopower of $Mo_4Ru_2Se_8$ which is n-type ($S<0$) over most of the temperature range.

to Z (vide supra). The thermal hysteresis in the measured thermopower is likely due to surface oxidation of the sample during the measurement, or degradation of the electrical contacts. In calculating PF the data taken on warming were used.

The measured resistivity of $Ti_{0.3}Mo_5RuSe_8$ increases slowly with temperature up to about 1000 K, at which point it begins to decline. The thermopower is positive indicating conduction dominated by holes, and achieves a maximum value at about the same temperature as the resistivity. This behavior suggests that $Ti_{0.3}Mo_5RuSe_8$ may be described as a heavily doped semiconductor, with the decline in resistivity and thermopower seen at the highest temperatures attributed to the onset of intrinsic behavior.

For comparison, data for some other Chevrel phase materials are also included in the plots. These include: the unfilled compound Mo_6Se_8, the unfilled mixed Mo/Ru cluster compound $Mo_4Ru_2Se_8$, and the Ti-filled pure Mo cluster compound $Ti_{0.9}Mo_6Se_8$. When compared to the parent compound Mo_6Se_8, the influence of fillings and cluster core substitutions (both increasing the VEC) on the TE properties are apparent in Fig. 3. Inspection of the PF plot also shows that the combination of filling and substitutions used in $Ti_{0.3}Mo_5RuSe_8$ is more effective than just filling with Ti ($Ti_{0.9}Mo_6Se_8$) or just substituting Ru ($Mo_4Ru_2Se_8$). However, this material does not perform as well as $Cu_{3.1}Mo_6Se_8$, which has PF $\sim 6\,\mu W/K^2\,cm$ at 1000 K [5].

Goldsmid and Sharp have shown that the band gap of a material can be estimated from the maximum in the S vs. T plot [26]. They derived the expression $E_{gap} \approx 2S_{max}T$, where T is the temperature at which the maximum thermopower S_{max} is realized. They note that this method typically gives errors of about 5–20%. Applying this equation to the data presented in Fig. 3 gives an estimated band gap of 0.16 eV for $Ti_{0.3}Mo_5RuSe_8$, 0.32 eV for $Mo_4Ru_2Se_8$, and 0.08 eV for $Ti_{0.9}Mo_6Se_8$. It is not surprising that the gap of $Ti_{0.3}Mo_5RuSe_8$ lies between those of the fully Ru-substituted phase $Mo_4Ru_2Se_8$ and the Ti-filled phase $Ti_{0.9}Mo_6Se_8$. The variation in the band gaps shows that these fillings and substitutions do more than simply add electrons to the clustermetal d-orbital-based conduction band, but in fact alter the band structure near the Fermi level.

4. Conclusions

The new Chevrel phase $Ti_{0.3}Mo_5RuSe_8$, incorporating both filling atoms and cluster core substitutions, has been synthesized, and the structure of its Mo_5RuSe_8 framework refined. Although the location of the Ti atoms could not be determined from the powder X-ray diffraction data, their influence on the Chevrel phase framework was observed. This was made possible by the Rietveld refinement of the structure of the unfilled phase Mo_5RuSe_8. The observed changes in the M–M distances in the octahedral cluster core and the M–Se distances in the M_6Se_8 unit caused by the Ti filling follow the general trends that have been previously observed in Chevrel phase compounds. The measured thermoelectric properties of $Ti_{0.3}Mo_5RuSe_8$ show it to behave like a heavily doped semiconductor, and a band gap of 0.16 eV was estimated from the

thermopower data. Although its high temperature thermoelectric properties are not as good as those of the best Chevrel phase thermoelectric material ($Cu_{3.1}Mo_6Se_8$), it does outperform both $Ti_{0.9}Mo_6Se_8$ and $Mo_4Ru_2Se_8$. This demonstrates how a combination of both filling and cluster core substitutions can lead to improved thermoelectric materials.

Supporting information

Further details of the crystal structure investigation for Mo_5RuSe_8 can be obtained from the Fachinformationszentrum Karlsruhe, 76344 Eggenstein-Leopoldshafen, Germany (fax: +49 7247 808 666; e-mail: crysdata@fiz.karlsruhe.de) on quoting the depository number 416365.

Acknowledgments

This work was funded by NASA/JPL. We thank John Hunt for assistance with the electron microprobe facility, which is part of the Cornell Center for Materials Research (MRSEC Grant DMR-0520404). Portions of this work were carried out by the Jet Propulsion Laboratory, California Institute of Technology, under contract with NASA.

References

[1] R. Chevrel, M. Sergent, J. Prigent, J. Solid State Chem. 3 (1971) 515.
[2] O. Fischer, M.B. Maple (Eds.), Topics in Current Physics: Superconductivity in Ternary Compounds I, Springer, Berlin, 1982.
[3] A. Perrin, R. Chevrel, M. Sergent, O. Fischer, J. Solid State Chem. 33 (1980) 43.
[4] T. Caillat, J.-P. Fleurial, J. Phys. Chem. Solids 59 (1998) 1139.
[5] T. Caillat, J.-P. Fleurial, G.J. Snyder, Solid State Sci. 1 (1999) 535.
[6] T. Hughbanks, R. Hoffmann, J. Am. Chem. Soc. 105 (1983) 1150.
[7] C. Roche, R. Chevrel, A. Jenny, P. Pecheur, H. Scherrer, S. Scherrer, Phys. Rev. B 60 (1999) 16442.
[8] K. Yvon, E. Paoli, Solid State Commun. 24 (1977) 41.
[9] R.R. Heikes, R.W. Ure Jr., Thermoelectricity: Science and Engineering, Interscience Publishers, New York, London, 1961.
[10] G.J. Snyder, T. Ursell, Phys. Rev. Lett. 91 (2003) 148301.
[11] G.J. Snyder, T. Caillat, Mater. Res. Soc. Symp. Proc. 793 (2004) 37.
[12] G.D. Mahan, B. Sales, J. Sharp, Phys. Today 50 (1997) 42.
[13] J.M. Tarascon, J.V. Waszczak, G.W. Hull Jr., F.J. DiSalvo, L.D. Blitzer, Solid State Commun. 47 (1983) 973.
[14] (a) S. Belin, R. Chevrel, M. Sergent, J. Solid State Chem. 145 (1999) 159;
(b) S. Belin, L. Burel, R. Chevrel, M. Sergent, Mater. Res. Bull. 35 (2000) 151.
[15] J. Rodriguez-Carvajal, FULLPROF.2k version 3.30 June 2005, ILL (unpublished).
[16] J.A. McCormack, J.-P. Fleurial, Mater. Res. Soc. Symp. Proc. 234 (1991) 135.
[17] C. Wood, D. Zoltan, G. Stapfer, Rev. Sci. Instrum. 56 (1985) 719.
[18] (a) D.G. Hinks, J.D. Jorgensen, H.-C. Li, Phys. Rev. Lett. 51 (1983) 1911;
(b) R. Cerny, K. Yvon, M. Wakihara, P. Fischer, J. Alloys Compd. 209 (1994) L29;
(c) C.L. Chang, Y.K. Tao, J.S. Swinnea, H. Steinfink, Acta Crystallogr. C 43 (1987) 1461.
[19] H.L. Schick, Chem. Rev. 60 (1960) 331.
[20] J. Tobola, P. Pecheur, H. Scherrer, S. Kaprzyk, Y. Ohta, Y. Matsumura, J. Phys: Condens. Matter 15 (2003) L655.
[21] L.S. Selwyn, W.R. McKinnon, J. Phys. C: Solid State 20 (1987) 5105.
[22] A. Mancour-Billah, R. Chevrel, J. Solid State Chem. 170 (2003) 281.
[23] S. Belin, R. Chevrel, M. Sergent, J. Solid State Chem. 155 (2000) 250.
[24] O. Bars, J. Guillevic, D. Grandjean, J. Solid State Chem. 6 (1973) 48.
[25] F.J. Berry, C. Gibbs, J. Solid State Chem. 109 (1994) 22.
[26] H.J. Goldsmid, J.W. Sharp, J. Electron. Mater. 28 (1999) 869.
[27] A.M. Schmidt, M.A. McGuire, F. Gascoin, G.J. Snyder, F.J. DiSalvo, J. Alloys Compd., in review.